Utrecht University

Finding Optimal Spaces for Nature-Based Solutions in Urban Areas

An approach with computer vision, trigonometry
and geospatial analysis

Jelle Tuik

Master Applied Data Science
Graduate School of Natural Sciences

August 19, 2024

Contents

1 Introduction

Climate change poses significant challenges to urban growth both within and beyond city boundaries(Liu et al., 2022). Cities experience the adverse effects of climate change through impacts on human health, livelihoods, and main infrastructure (Lee et al., 2023). Moreover, Urban areas are susceptible to its effects, notably through the exacerbation of the urban heat island (UHI) phenomenon. This phenomenon is defined by elevated temperatures within cities compared to their surrounding rural areas (Koch et al., 2020). The temperature differential can be substantial, with some urban centers experiencing up to 10 degrees Celsius higher temperatures than their rural counterparts. Contributing factors are the proliferation of heat-generating activities, the predominance of materials with high thermal mass and low albedo in urban infrastructure (Galagoda et al., 2018), and the relative scarcity of green and blue spaces within city limits. Urban structures, majorly composed of materials like concrete, asphalt, and metal, exhibit enhanced heat absorption and re-radiation properties (Rizwan, Dennis, and Liu, 2008). This thermal behavior is evident during nocturnal hours, when artificial surfaces in urban environments demonstrate a markedly slower rate of cooling compared to natural elements.

1.1 Nature-Based Solutions

To address these challenges, the concept of Nature-based Solutions has been suggested (Liu et al., 2022). Nature-based solutions (NbS) are strategic interventions that uses and connect the distinctive capabilities of natural systems to tackle environmental, social, and economic challenges Commission, Research, and Innovation, 2015. These solutions draw on the principles of ecological design and sustainability. NbS stimulates the resilience of the environment, together with human development goals and adaptability to local contexts. There is no principal archetype or model that illustrates a typical NbS. Nevertheless, most projects documented by the European Investment Bank (EIB) in 2023 mainly implied the establishment of new parks and gardens, alongside retrofitting green infrastructure on walls and roofs into existing urban environments.

Growing awareness about environmental hazards for cities has been observed at different levels of the public and private sector (Seddon et al., 2020; Lee et al., 2023). Despite the benefits and cost-effectiveness of NbS, governments are facing multiple barriers. Dorst et al., 2022 identified barriers that are fundamental for limited implementation of NbS in The Netherlands. These include competition for urban space among stakeholders due to high urban densities and a lack of sufficient public resources – Although the public sector guides the private sector in selecting locations for housing development, the plans are predominantly short-term and involve only tasks that are considered as a high-priority by the government (Koninkrijksrelaties, 2024). Meanwhile, NbS require long-term planning to maintain the spaces (Liu et al., 2022). Several studies found that local governments are subjected to technical difficulties. More specific, knowledge gaps in the use of assessment tools and data restrictions (Bush,

2020; Dorst et al., 2022). Municipalities in The Netherlands are increasingly seeking more sophisticated instruments to address the challenges posed by climate change (Heleen Mees and Dieperink, 2018). However, there is still a knowledge gap between what these tools reveal about the impacts of climate change on specific municipalities and the actual implementation of practical solutions. Consequently, considering the effectiveness of green walls, development of a robust methodology for identifying suitable sites for NbS is valuable. Furthermore, the automation of this process and applying standardised variables is imperative to ensure applicability and transferability across other urban contexts in The Netherlands. Previous studies attempting to estimate building dimensions merely focused on calculating proportional relationships, rather than deriving absolute measurements in standardised units of length such as meters (Zarghami et al., 2019). This leads to the research question.

1.1.1 Research Question

To what extent can facades be correctly measured in real-world scale for applying vertical gardens?

1.2 Related work

The integration of AI-driven tools in urban planning is considered helpful in informing and guiding urban policy to facilitate urban transformation (Kamrowska-Załuska, 2021; Son et al., 2023). The conducted literature review of Kamrowska-Załuska, 2021 demonstrates that when big data analytics and AI-related tools are applied in urban planning, they provide a more accurate representation of a city's functional and spatial complexities. Notably, when AI is applied in early stages of urban planning, it improves the chances to wider adoption (Son et al., 2023). Depending on the task, AI-tools and data sources differ. However, Biljecki and Ito, 2021 concluded in their research from 2021 that street view images (SVIs) have become an important source for data collection in spatial and urban analytics. In their analysis, they found that most of the research relies on SVI data from Google. In addition, research that aimed to identify and calculate the amount of greenery from street-level, used predominantly semantic segmentation. In 2022, Qian et al., 2022 addressed the lack of large-scale, accurate geospatial data on Roadside Noise Barriers (RNBs) in China, that hinders effective urban planning and sustainable city development. Utilizing a geospatial artificial intelligence framework and street view imagery, the researchers created a vectorized dataset of RNBs. They employed intensive sampling of the road network from OpenStreetMap and analyzed 6 million Baidu Street View images using convolutional neural networks that incorporate image context (IC-CNNs) through ensemble learning. Results from evaluation suggested that the RNB dataset has a high quality and can be applied as an accurate and reliable dataset for large-scale urban studies. The method provided may be useful for this research. In 2023, Li et al., 2023 applied a computer vision technique for mapping tree inventory in cities from street view images. Besides identifying

3

the tree species, the algorithm was able to estimate the depth of each pixel in the image to assess the physical dimensions. They concluded in their research that the adapted method had an higher accuracy in tree recognition compared to existing methods. Their method could be helpful in finding potential locations for NbS, particularly for urban tree placement. In their study in land price estimation, Zhao et al., 2023 developed a new approach that implemented deep learning to consider both streetscape and human subjective perception factors. Land prices were estimated directly from street view images. In their analysis, they extracted the results of semantic segmentation and perception scores from these images and integrate them with land price data. This approach achieved an accuracy of 77.99% in predicting land prices based solely on street views. In 2024, Sánchez and Labib, 2024 developed a methodology to estimate the Green View Index (GVI) using open-source street view images (SVIs). They demonstrated the applicability of freely accessible Mapillary data for calculating GVI. In areas with limited SVI availability, they employed the Normalized Difference Vegetation Index (NDVI) derived from satellite imagery. Previous research regarding building detection mainly focused on the geometric shape, while semantic attributes - e.g., house number and building name - are not attended (Sun et al., 2023). To overcome this, (Sun et al., 2023) developed a method that effectively extracts information from street-view images and integrates it with OpenStreetMap (OSM) building footprints. This workflow consists of three steps: first, employing deep neural networks to recognize information from the images; second, clustering this information to categorize it into predefined attribute classes; and third, integrating the categorized information into OSM building footprints to enhance their semantic attributes. This method could be useful in ensuring that potential NbS locations identified through AI align accurately with the correct building and geographical location. Also, this may improve the precision of urban planning initiatives.

2 Method

This study had an interdisciplinary approach by integrating computer vision, trigonometric principles, and geospatial analysis, to address the research question: To what extent can facades be correctly measured in real-world scale for applying vertical gardens?

The research was conducted within a 2.22 km^2 area in the eastern region of The Netherlands, in the municipality of Zwolle. This area was selected as the study area due to:

1. A mixed bag of building and house typologies.

2. Sufficient and reliable data sets that are also available for other Dutch cities.

3. Architectural characteristics representative of other Dutch, historic urban centers.

Importantly, these factors aims to contribute to the applicability of the methodology, as the municipality of Zwolle constitute as a representative sample for broader urban contexts within The Netherlands. This research proposed to develop and validate a methodological framework for accurately assessing potential vertical garden sites in urban settings, with implications for sustainable urban development and green infrastructure planning. Figure 1 shows a schematic representation of the method divided in four steps. The subsequent sections provide a detailed description of these methodological processes.
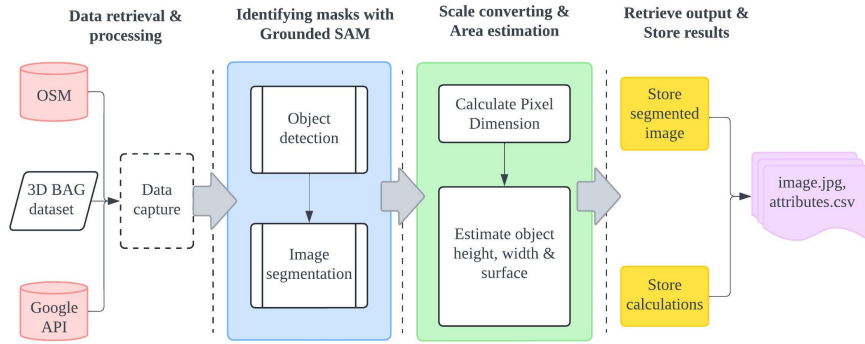

Figure 1: Flowchart representing the method in four subsequent stages

2.1 Data Retrieval & Processing

Data acquisition was conducted through the Google Maps API, with two request types. The initial phase of the process concerned utilising the API to retrieve metadata of SVIs. This approach aided adaptive error handling without exhausting quota limits, as the charging model of Google applies only to the static SVI itself (LLC, n.d.). Moreover, this method was selected due to the homogeneous quality, availability, and common use in similar research (Biljecki and Ito, 2021). In addition, the functionality to query on coordinates, heading, and field of view in the Google ecosystem improved processing efficiency for retrieving static SVIs.

Building morphology, including shapes and height characteristics, was obtained from the 3D Basisregistratie Adressen en Gebouwen (3D BAG) dataset (Peters et al., 2022). This data was instrumental for distance calculations and validation purposes. The road network data was extracted from OpenStreetMap (OSM) by querying road features within the spatial extent of the study area.

2.1.1 Data Capture

An iterative method was constructed for efficiency - and avoiding prior bias - in finding potential facades, illustrated as a data flow diagram in figure 2. Uni-

form sampling was performed on the relevant road network of the study area. Sample points were generated at 10-meter intervals along the roads. Each generated point was queried on the Google SVI Metadata API, and collected unique panorama IDs, with corresponding latitude and longitude coordinates. Duplicates were removed before storing the panorama metadata. Building polygons were decomposed into individual edges that represented a potential facade. For each SVI point, proximity analysis was performed by determining the nearest facade. This analysis had the following steps:

1. Calculate the perpendicularity distance from the point to the facade.

2. Compute the angle between the facade vector and the point vector.

3. Assessing the centrality of the point projection along the facade.

To obtain the best point when there were multiple candidate points for a building, a composite score was derived by assessing: (1) Distance from the facade, (2) deviation from perpendicularity (90-degree angle), and (3) centrality along the facade length.

2.2 Identifying masks with Grounded SAM

Identifying objects and generating masks was performed with the Grounded Segment Anything model. It integrates the zero-shot detection capabilities - a paradigm in machine learning wherein an AI-model is trained to recognise and categorise objects without prior exposure to exemplars from those specific categories (Bergmann, 2024) - of Grounding DINO with the adaptable image segmentation functionality of Segment Anything (Ren et al., 2024). This combination simplifies the detection and precise segmentation of objects within visual stimuli through text prompts. Regarding this research, the integrated approach boosted efficiency since only a natural language prompt and image were needed as input.

2.2.1 Object Detection

First, Grounding DINO was employed; an object detection model developed by Liu et al. (2023). This model has high accuracy at identifying objects within an image based on textual queries. In this stage, different prompts were evaluated on their detection accuracy. While 'facade' may be seen as a rational input - since it is the objective of the research - better performance in detection accuracy was achieved with the prompt 'building'. A plausible explanation for this is the labeled training data, where 'building' could be more common than 'facade'. Grounding DINO then analyzes the street view images and returns valid detections as bounding boxes, with each accompanied by a corresponding label and an accuracy score.
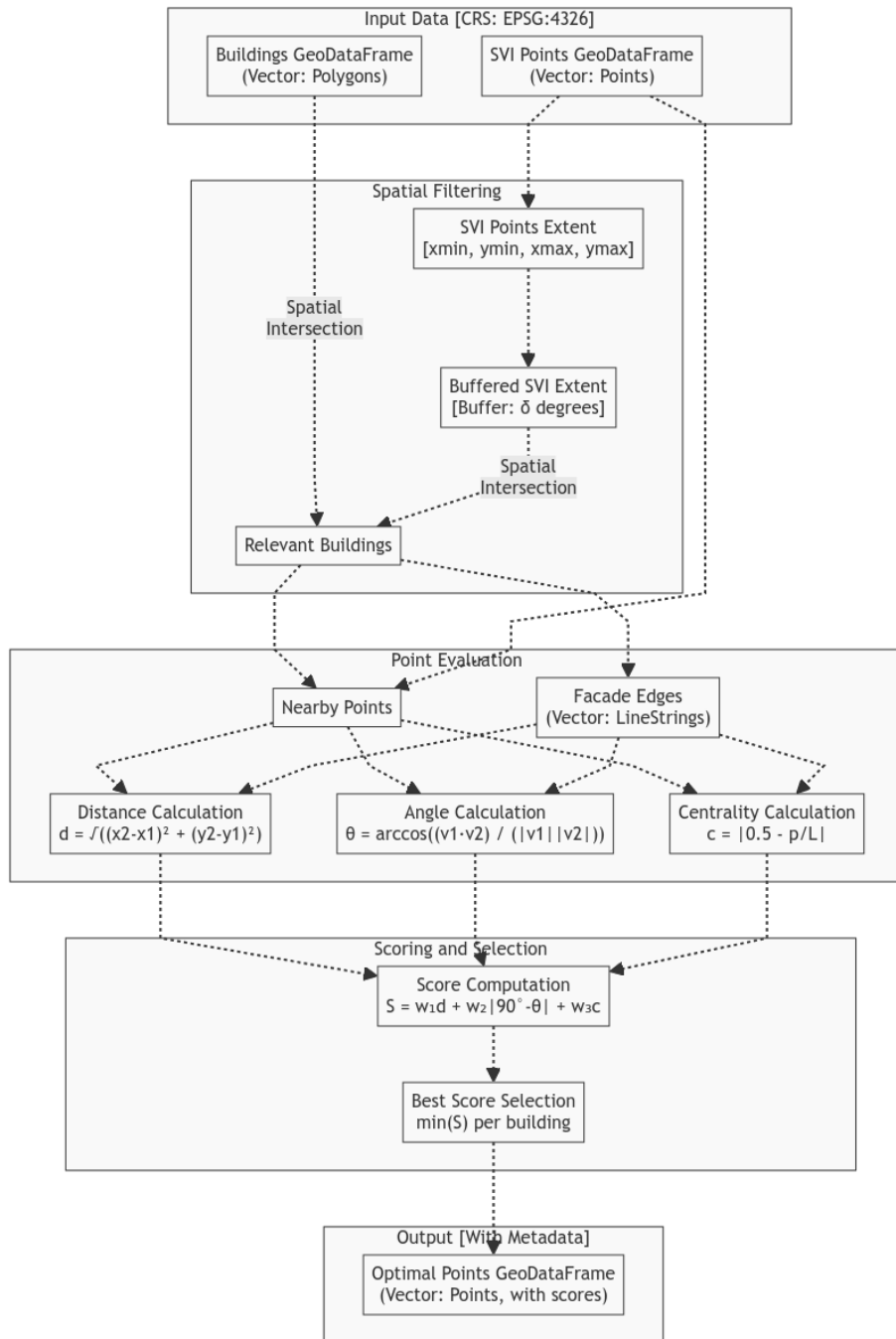
Figure 2: Data flow diagram of Data Capture

2.2.2   Image Segmentation

Following the object detection phase, bounding box outputs are pulled as inputs for the Segment Anything Model (SAM), developed by Kirillov et al. (2023). SAM, designed and trained to be adaptable to point, boxes and text prompts, performs the segmentation task. It refines the initial bounding box detections from Grounding DINO and creates precise pixel-level masks of the buildings. The segmentation output is then used for dimensional analysis, to allocate boundaries of each building, including architectural features.

2.3   Scale Converting & Area Estimation

Masks and attributes for building objects were initially obtained through image segmentation. These masks represented the outline of the building within the image. To transition from pixel-based data to real-world dimensions, a conversion was established as a factor between pixel size and actual measurements. The transformation of pixel-based measurements from images into real-world scalar quantities requires a known reference length (Yan and Huang, 2022). As mentioned, the coordinates of the SVI and building were used to calculate the distance and served as a reference length. The equation for determining pixel scale, was adapted from Calter's 'façade measurement by trigonometry' method (Calter, 2014). It was extended by considering the camera height in calculations. Equation 1 and 2 were applied for scale conversion.

$$h_p = \frac{2d\tan(\frac{\theta_v}{2})}{H} \tag{1}$$

$$w_p = \frac{2d\tan(\frac{\theta_h}{2})}{W} \tag{2}$$

Where:

- h_p, w_p are the height and width of a pixel in real-world units, respectively
- d is the distance from the camera to the object
- θ_v, θ_h are the vertical and horizontal field of view in radians, respectively
- H, W are the height and width of the image in pixels, respectively

$$A = n_p \cdot (h_p \cdot w_p) \tag{3}$$

Where:

- A is the total area
- n_p is the number of pixels in the mask (pixel count)
- h_p is the height of a pixel in real-world units
- w_p is the width of a pixel in real-world units

2.3.1 Surface Estimation

Dimensional analysis commenced with the transformation of the building mask into a binary object. This binary representation aid identification of the object boundaries within the image. Equation 3 determined the minimum and maximum x and y coordinates where the mask held a 'true' value (i.e., whether presence of the object or not). Coordinate ranges of the image, when multiplied by equation 1, yield the estimated height and width of the building in real-world units. To calculate the gross area of the building, valid points were summed within the mask (merely counting the pixels representing the building) and multiply this sum by the area of a single pixel in real-world units, as shown in equation 3. Precision of the surface area estimation was established by accounting for architectural elements that would not be suitable for vertical garden. Considering image resolution and common building features, the segmentation process only generated separate masks for windows and doors. By subtracting the areas represented by these features from the gross area, the net surface area of the building was calculated.

2.4 Constraints & Validations

The selection of a limited number of sampling points (n = 38) was driven by significant computational constraints inherent in the processing of large-scale image datasets. The full dataset compromises approximately 12.000 SVIs and presents a substantial computational time when processed on conventional CPU architecture. Iteration time of applying image segmentation, coupled with the volume of data, would result in immoderate long processing time. The limitation in computational resources led to the decision to employ a manual selection process for sampling points. While this approach introduces potential selection bias (Zhang and Zhu, 2018), it allows for a proof-of-concept demonstration of the methodology within the available resources. Nevertheless, manual selection mirrored the criteria - i.e., perpendicularity to road, horizontal angle to building - that would be applied when following the automated approach, thus maintaining consistency with the intended methodology.

3 Results

This section presents the results obtained from the sequential stages of the study. It is important to note that full automatic processing was implemented up to the image segmentation phase. Subsequent results presented herein are derived from the manually selected subset of data. This methodological approach was bound by computational constraints, as discussed in the previous section.

3.1 Data Capturing Results

In the first step, 22.326 points were generated in the study area. After preprocessing, 12.786 points that represents an SVI were returned. Figure 3 shows a

map of the processed points as orange dots.

Figure 3: Map showing potential SVI locations as orange dots

3.2 Segmentation Results

A juxtaposition of a valid process is presented in figure 4. With (a) as original
retrieved SVI with correct orientation of an urban structure. And (b) The
processed counterpart that illustrates the application of the segmentation, with
detected building elements and estimated dimensions annotated.

Illustration of a partially valid segmentation process is in Figure 5. (a) The
original Street View Image (SVI) presenting a multi-story office building. And
(b) The result of the segmentation model. The figure exemplifies a partially suc-
cessful segmentation result. The applied trigonometry function demonstrates
accuracy in estimating the overall building height, when compared with the
object height from the 3D BAG dataset. However, it encounters difficulties
in identifying all relevant windows, which occurs more often for this type of
structures, and for all building types when distance is increased from the view-
point. Despite these constraints, the ability of the method to accurately gauge
the building height may suggests that certain volumetric estimations remain
reliable, even when finer architectural details prove elusive.
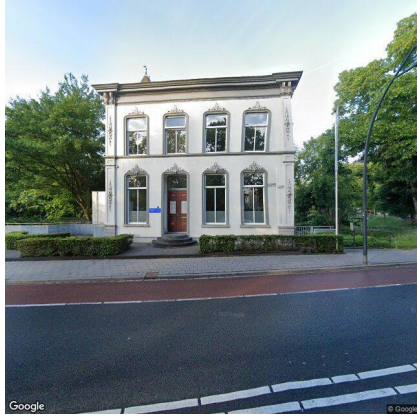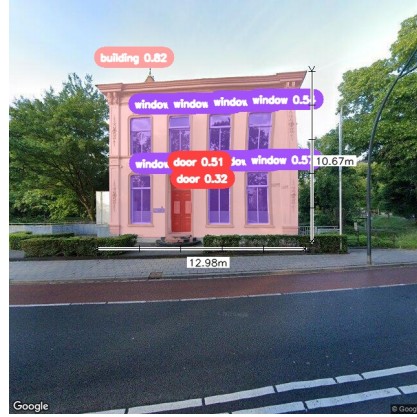
(a) Retrieved image   (b) Processed image

Figure 4: Example of a valid segmentation process

(a) Retrieved image   (b) Processed image

Figure 5: Example of a partially valid segmentation process

3.3 Validation

The analysis reveals a positive correlation between distance and estimation error across all three height measures from the 3D BAG dataset. The strongest correlation is observed for the maximum height error (r = 0.3012), followed by the median height error (r = 0.2814), with the minimum height error showing the weakest, albeit still positive, correlation (r = 0.2291). These positive correlations could suggest that as the distance from the building increases, there is a tendency for the magnitude of estimation errors to increase as well. The strength of these correlations, while not robust, suggests a non-negligible influence of distance on estimation accuracy. Interestingly, the hierarchy of correlation strengths aligns with the vertical positioning of the measured points on the building facade. The strongest correlation for maximum height errors may be attributed to the challenges in accurately discerning the topmost point of a structure from increased distances. Conversely, the weaker correlation for minimum height errors could be due to the relative stability of ground-level reference points across various distances. It should be noted that, building geometry, environmental conditions, or algorithmic limitations, may also contribute to the observed error patterns. The moderate strength of these correlations suggests that while distance is a significant factor in estimation accuracy, it is not the sole determinant. The analysis of height estimation accuracy across distances

Error Type	Correlation with Distance
Error (Maximum Height)	0.3012
Error (Median Height)	0.2814
Error (Minimum Height)	0.2291

Table 1: Pearson correlation coefficients between distance and height estimation errors

shows a logic and linear pattern of increasing error as the distance from the subject building increases. Table 2 presents the Mean Absolute Percentage Error (MAPE) for maximum, median, and minimum height estimates across three distance ranges. As evident from the data, the MAPE for all height measures (maximum, median, and minimum) demonstrates an upward trend with increasing distance. For distances between 0-20 meters, the MAPE ranges from 7.23% for maximum height to 13.62% for minimum height. This error margin expands for measurements taken at 20-40 meters, with MAPE values ranging from 8.15% to 13.87%. The most pronounced errors are observed at distances exceeding 40 meters, where the MAPE reaches 9.72% for maximum height and 14.98% for minimum height estimates. Notably, the minimum height estimates consistently exhibit the highest MAPE across all distance ranges that may suggest a systematic overestimation bias for this parameter. Conversely, maximum and median height estimates show comparable levels of error, with slightly lower MAPE values than those for minimum height. The increasing MAPE with distance underscores the importance of proximity in achieving accurate height estimations.

This trend may be attributed to factors such as diminishing visual resolution, increased perspective distortion, or limitations in the estimation algorithm at greater distances. Finally, it shows the decreasing sample size as distance increases, which may introduce some uncertainty in the error estimates for the larger distance ranges.

Distance (meters)	MAPE Max Height	MAPE Median Height	MAPE Min Height	Sample Size
0–20	7.23%	7.54%	13.62%	18
20–40	8.15%	8.40%	13.87%	13
40+	9.72%	10.35%	14.98%	7

Table 2: Mean Absolute Percentage Error (MAPE) for height estimates by distance range

4 Discussion

The study presents an approach to measure building facades for potential vertical garden applications using a combination of street view imagery (SVI), computer vision techniques, and geospatial analysis. This method demonstrates promise in automating the process of identifying suitable locations for nature-based solutions (NbS) in urban environments, addressing the growing need for climate change adaptation strategies in cities (Liu et al., 2022; Lee et al., 2023).

4.1 Methodology Effectiveness

The multi-step methodology with data retrieval, image segmentation, scale conversion, and area estimation, shows potential for large-scale urban analysis. The use of Google Street View API for data acquisition proves efficient, providing a consistent and widely available data source. The integration of Grounded Segment Anything Model (SAM) for object detection and segmentation demonstrates high segmentation accuracy which could be useful in urban planning applications that aligns with recent trends in AI-driven urban analytics (Kamrowska-Załuska, 2021; Son et al., 2023).

4.2 Accuracy and Limitations

The results indicate that the method is capable of producing reasonably accurate estimations of building dimensions for buildings at closer ranges. The analysis reveals a positive correlation between distance and estimation error, with the strongest correlation observed for maximum height error (r = 0.3012). This may suggest that the accuracy of the method decreases as the distance from the building increases.

The Mean Absolute Percentage Error (MAPE) analysis further supports this observation, showing an upward trend in error rates as distance increases. For instance, the MAPE for maximum height estimates ranges from 7.23% at 0-20 meters to 9.72% at distances exceeding 40 meters.

Interestingly, the minimum height estimates consistently exhibit the highest MAPE across all distance ranges. It could be assumed that this is a systematic overestimation bias. This could be due to challenges in accurately identifying the ground level in street view images which is possibly caused by obstructions like trees, cars or perspective distortions.

4.3 Implications for urban planning

The developed method can be used as a tool within urban planning as a tool for cost estimation of green walls per object - because of the use of real-world scale - and the implementation of NbS. By automating the process of identifying suitable facades for vertical gardens, this approach could greatly enhance the chance of convincing stakeholders in urban greening initiatives. The ability to assess large urban areas for potential green infrastructure sites could accelerate the adoption of NbS, contributing to climate change adaptation and mitigation efforts in cities (Commission, Research, and Innovation, 2015; Seddon et al., 2020).

However, the observed limitations, particularly the decrease in accuracy with distance - and computation resources needed -, suggest that the method may be most reliable for assessing buildings in close proximity to the street. This could potentially bias the selection of suitable sites towards buildings closer to roads, which may not always align with optimal locations for vertical gardens from an ecological or urban planning perspective.

4.4 Computational Challenges

The study encountered significant computational constraints, necessitating a manual selection process for a subset of data points. While this approach allowed for a proof-of-concept demonstration, it introduces potential selection bias and limits the scalability of the method. Addressing these computational challenges will be crucial for the practical application of this methodology at a city-wide scale, a concern echoed in similar large-scale urban studies (Qian et al., 2022).

4.5 Future work

Future research could focus more on the improvement and scaling of calculation resources that emerged during this study. Other possible improvements could be:

- Enhance accuracy of measurements for buildings at greater distances, perhaps through the development of distance-based correction factors or improved image processing techniques.

- Address the systematic overestimation of minimum height, which could involve refining the ground level detection algorithms.

- Exploring ways to reduce computational demands, enabling the processing of larger datasets and facilitating city-wide analyses.

- Developing methods to account for other factors relevant to vertical garden suitability, such as sunlight exposure, wall material, and structural integrity.

5 Conclusion

This study demonstrated an automatic approach to measure building facades for potential vertical garden applications using street view imagery and computer vision techniques. The methodology shows promising accuracy for buildings in close proximity to the viewpoint, but with increasing error rates at greater distances. Limitations and potentials of the current approach can be seen in the positive correlation between distance and estimation error, along with the increasing MAPE values for greater distances. While the method offers a valuable tool for rapidly assessing green walls with trigonometry, the segmentation of an image takes more time, but could be improved with a more lightweight and tuned segmentation model. The computational challenges encountered could therefore be solved, but needs more efficient processing methods to enable city-wide analyses. Despite these limitations, the developed methodology represents a step towards automating the identification of suitable sites for vertical gardens and other urban greening initiatives to address key barriers identified in previous research (Dorst et al., 2022; Bush, 2020).

Future research could focus on improving measurement accuracy at greater distances, which is useful for skyscraper building environments, like Rotterdam. And with addressing systematic biases that improves computational efficiency. Additionally, integrating this approach with other urban planning tools and data sources could lead to more comprehensive and accurate assessments of urban environments for nature-based solutions (Sun et al., 2023).

In conclusion, while further refinement is needed, the method of this study aimed to lay a foundation for more efficient and data-driven urban greening strategies and the implementation of nature-based solutions in cities. And, therefore, hoping to indirect contribute to urban resilience for climate change (Heleen Mees and Dieperink, 2018; Liu et al., 2022).

References

Bergmann, D (Jan. 2024). *What is Zero-Shot Learning?* URL: `https://www.ibm.com/topics/zero-shot-learning`.

Biljecki, Filip and Koichi Ito (Nov. 2021). "Street view imagery in urban analytics and GIS: A review". In: *Landscape and urban planning* 215, p. 104217. DOI: `10.1016/j.landurbplan.2021.104217`. URL: `https://doi.org/10.1016/j.landurbplan.2021.104217`.

Bush, Judy (June 2020). "The role of local government greening policies in the transition towards nature-based cities". In: *Environmental innovation and societal transitions* 35, pp. 35–44. DOI: `10.1016/j.eist.2020.01.015`. URL: `https://doi.org/10.1016/j.eist.2020.01.015`.

Calter, Paul A. (Apr. 2014). *Façade measurement by trigonometry*, pp. 261–269. DOI: `10.1007/978-3-319-00137-1\{_}18`. URL: `https://doi.org/10.1007/978-3-319-00137-1_18`.

Commission, European, Directorate-General for Research, and Innovation (2015). *Towards an EU research and innovation policy agenda for nature-based solutions re-naturing cities – Final report of the Horizon 2020 expert group on 'Nature-based solutions and re-naturing cities' – (full version)*. Publications Office. DOI: `doi/10.2777/479582`.

Dorst, Hade et al. (Apr. 2022). "What's behind the barriers? Uncovering structural conditions working against urban nature-based solutions". In: *Landscape and urban planning* 220, p. 104335. DOI: `10.1016/j.landurbplan.2021.104335`. URL: `https://doi.org/10.1016/j.landurbplan.2021.104335`.

Galagoda, R.U. et al. (Aug. 2018). "The impact of urban green infrastructure as a sustainable approach towards tropical micro-climatic changes and human thermal comfort". In: *Urban forestry urban greening* 34, pp. 1–9. DOI: `10.1016/j.ufug.2018.05.008`. URL: `https://www.sciencedirect.com/science/article/abs/pii/S1618866718301687`.

Heleen Mees, Niels Tijhuis and Carel Dieperink (2018). "The effectiveness of communicative tools in addressing barriers to municipal climate change adaptation: lessons from the Netherlands". In: *Climate Policy* 18.10, pp. 1313–1326. DOI: `10.1080/14693062.2018.1434477`. eprint: `https://doi.org/10.1080/14693062.2018.1434477`. URL: `https://doi.org/10.1080/14693062.2018.1434477`.

Kamrowska-Załuska, Dorota (2021). "Impact of AI-Based Tools and Urban Big Data Analytics on the Design and Planning of Cities". In: *Land* 10.11. ISSN: 2073-445X. DOI: `10.3390/land10111209`. URL: `https://www.mdpi.com/2073-445X/10/11/1209`.

Koch, Kyra et al. (Nov. 2020). "Urban heat stress mitigation potential of green walls: A review". In: *Urban forestry urban greening* 55, p. 126843. DOI: 10.1016/j.ufug.2020.126843. URL: https://doi.org/10.1016/j.ufug.2020.126843.

Koninkrijksrelaties, Ministerie van Binnenlandse Zaken en (Apr. 2024). *Toezicht op woningcorporaties*. URL: https://www.rijksoverheid.nl/onderwerpen/woning-verhuren/toezicht-op-woningcorporaties.

Lee, Hoesung et al. (2023). "IPCC, 2023: Climate Change 2023: Synthesis Report, Summary for Policymakers. Contribution of Working Groups I, II and III to the Sixth Assessment Report of the Intergovernmental Panel on Climate Change [Core Writing Team, H. Lee and J. Romero (eds.)]. IPCC, Geneva, Switzerland." In.

Li, Dongwei et al. (Mar. 2023). "Establishing a citywide street tree inventory with street view images and computer vision techniques". In: *Computers, environment and urban systems* 100, p. 101924. DOI: 10.1016/j.compenvurbsys.2022.101924. URL: https://doi.org/10.1016/j.compenvurbsys.2022.101924.

Liu, Yuexin et al. (June 2022). "Nature-based solutions for urban expansion: Integrating ecosystem services into the delineation of growth boundaries". In: *Habitat international* 124, p. 102575. DOI: 10.1016/j.habitatint.2022.102575. URL: https://doi.org/10.1016/j.habitatint.2022.102575.

LLC, Google (n.d.). *Street View Image metadata*. URL: https://developers.google.com/maps/documentation/streetview/metadata.

Peters, Ravi et al. (2022). *Automated 3D reconstruction of LoD2 and LoD1 models for all 10 million buildings of the Netherlands*. English. DOI: 10.14358/PERS.21-00032R2.

Qian, Z. et al. (2022). "Vectorized dataset of roadside noise barriers in China using street view imagery". In: *Earth System Science Data* 14.9, pp. 4057–4076. DOI: 10.5194/essd-14-4057-2022. URL: https://essd.copernicus.org/articles/14/4057/2022/.

Ren, Tianhe et al. (Jan. 2024). "Grounded SAM: Assembling Open-World models for diverse visual tasks". In: *arXiv (Cornell University)*. DOI: 10.48550/arxiv.2401.14159. URL: https://arxiv.org/abs/2401.14159.

Rizwan, Ahmed Memon, Leung Y.C. Dennis, and Chunho Liu (Jan. 2008). "A review on the generation, determination and mitigation of Urban Heat Island". In: *Journal of Environmental Sciences/Journal of environmental sciences* 20.1, pp. 120–128. DOI: 10.1016/s1001-0742(08)60019-4. URL: https://www.sciencedirect.com/science/article/abs/pii/S1001074208600194.

Seddon, Nathalie et al. (Jan. 2020). "Understanding the value and limits of nature-based solutions to climate change and other global challenges". In:

Philosophical transactions - Royal Society. Biological sciences 375.1794, p. 20190120. DOI: 10.1098/rstb.2019.0120. URL: https://doi.org/10.1098/rstb.2019.0120.

Son, Tim Heinrich et al. (July 2023). "Algorithmic urban planning for smart and sustainable development: Systematic review of the literature". In: *Sustainable cities and society* 94, p. 104562. DOI: 10.1016/j.scs.2023.104562. URL: https://doi.org/10.1016/j.scs.2023.104562.

Sun, Yao et al. (2023). "Artificial Intelligence based Building Attributes Enrichment in OpenStreetMap using Street-view Images". In: *Abstracts of the ICA* 6, p. 250.

Sánchez, Ilse Abril Vázquez and S.M. Labib (Feb. 2024). "Accessing Eye-level Greenness Visibility from Open-Source Street View Images: A methodological development and implementation in multi-city and multi-country contexts". In: *Sustainable cities and society*, p. 105262. DOI: 10.1016/j.scs.2024.105262. URL: https://doi.org/10.1016/j.scs.2024.105262.

Yan, Yizhen and Bo Huang (Oct. 2022). "Estimation of building height using a single street view image via deep neural networks". In: *ISPRS journal of photogrammetry and remote sensing* 192, pp. 83–98. DOI: 10.1016/j.isprsjprs.2022.08.006. URL: https://doi.org/10.1016/j.isprsjprs.2022.08.006.

Zarghami, Esmaeil et al. (Nov. 2019). "Assessing the oppressive impact of the form of tall buildings on citizens: Height, width, and height-to-width ratio". In: *Environmental impact assessment review* 79, p. 106287. DOI: 10.1016/j.eiar.2019.106287. URL: https://doi.org/10.1016/j.eiar.2019.106287.

Zhang, Guiming and A-Xing Zhu (July 2018). "The representativeness and spatial bias of volunteered geographic information: a review". In: *Annals of GIS* 24.3, pp. 151–162. DOI: 10.1080/19475683.2018.1501607. URL: https://doi.org/10.1080/19475683.2018.1501607.

Zhao, Chenbo et al. (Aug. 2023). "Quantitative land price analysis via computer vision from street view images". In: *Engineering applications of artificial intelligence* 123, p. 106294. DOI: 10.1016/j.engappai.2023.106294. URL: https://doi.org/10.1016/j.engappai.2023.106294.